RSC Advances

PAPER

View Article Online
View Journal | View Issue

Cite this: *RSC Adv.*, 2017, **7**, 56611

A novel organotrophic nitrate-reducing Fe(II)-oxidizing bacterium isolated from paddy soil and draft genome sequencing indicate its metabolic versatility†

Min Hu,‡[a] Pengcheng Chen,‡[abc] Weimin Sun,[a] Fangbai Li *[a] and Jianghu Cui[a]

The extensive application of fertilizers for growing rice results in a large input of nitrogen into paddy soils. During rice growth, iron is exposed to periodic transition under different redox conditions. Nitrate (NO_3^-) reduction coupled to Fe(II) oxidation (NRCFO) links the iron and nitrogen cycles. However, little is known about the biogeochemical mechanism and microorganisms involved in NRCFO in paddy soil. In the present study, we isolated an anaerobic, NO_3^--reducing Fe(II) oxidizer known as strain Paddy-1 from paddy soil. After 6 days of culture in 5 mM acetate, this strain reduced 97% of NO_3^- and oxidized 86% of Fe(II) from initial concentrations of 9.3 and 5.1 mM, respectively. A phylogenetic analysis of the 16S rRNA gene sequence placed strain Paddy-1 in a clade within the order *Rhodocyclales*. In accordance with other NRCFO species, Fe(III) oxides produced by strain Paddy-1 were in the form of amorphous Fe(III) oxides. The reported draft genome of strain Paddy-1 predicts the presence of genes involved in denitrification, outer membrane electron transport, and iron homeostasis as well as candidate Fe(II) oxidation genes. The physiological and genomic information on this strain provide a basis for investigating the mechanism of NRCFO in microorganisms from paddy soil.

Received 23rd August 2017
Accepted 12th December 2017

DOI: 10.1039/c7ra09328d

rsc.li/rsc-advances

1. Introduction

Iron and nitrogen are abundant elements in nature, and their redox cycling by microorganisms plays an important role in their overall biogeochemical cycles. Iron and nitrogen cycling are linked by nitrate (NO_3^-) reduction coupled to Fe(II) oxidation (NRCFO) through enzyme-mediated Fe(II) oxidation/NO_3^- reduction or chemical Fe(II) oxidation by NO_2^- produced during denitrification; or else by ammonium oxidation coupled to Fe(III) reduction.[1,2] NO_3^--dependent Fe(II) oxidation (NDFO) is the term used to describe this process. However, a valid method for differentiating abiotic (Fe(II) reacting with generated nitrite [NO_2^-]) from biotic (enzyme-mediated Fe(II) oxidation) effects in Fe(II) oxidation under NO_3^--reducing conditions is lacking. Additionally, the Fe(II) oxidases responsible for the formation of distinct NDFO species have not been identified, casting doubt on whether this process actually occurs.[3] Thus, Fe(II) oxidation could be NO_2^--induced under anoxic conditions, whereas NRCFO accounts for the undetermined biotic or abiotic effects in such processes.

Recent studies have investigated NRCFO in sediment and hydrothermal vents as well as in deep sea and freshwater wetland environments.[4–9] Long-term fertilization of paddy soils with nitrogenous manure for farming activities fosters nitrogen and iron biogeochemical cycles.[10] NO_3^- is produced from fertilizers enriched in ammonium (ammonium sulfate or urea) in the anoxic nitrification zone (3 mm soil depth),[11] in which NO_3^- replaces oxygen as the electron acceptor for Fe(II) oxidation.[1,12] NDFO in soil was first identified by measuring changes in the levels of nitrogen and iron species in soil depth profiles.[10] However, there is little information regarding NDFO in paddy soil ecosystems.

The availability of certain electron acceptors (SO_4^{2-}, NO_3^-, and Fe(III)) is a major determinant of the microbial community composition of paddy soils and sediments,[13] and could also affect the distribution and functionality of Fe(II)-oxidizing bacteria (FeOB), which can in turn influence the NRCFO process in paddy soil ecosystems. Many NRCFO species have been isolated from sediment and freshwater environments including *Acidovorax delafieldii* 2AN,[14] *Acidovorax ebreus* TPSY,[15] *Acidovorax* sp. BoFeN1,[16] *Azospira suillum* PS (formally *Dechlorosoma suillum*),[17] and *Pseudogulbenkiania* sp. 2002.[18] We previously

[a]*Guangdong Key Laboratory of Integrated Agro-environmental Pollution Control and Management, Guangdong Institute of Eco-Environmental Science & Technology, Guangzhou 510650, P. R. China. E-mail: cefbli@soil.gd.cn; Fax: +86 20 87024123; Tel: +86 20 37021396*

[b]*Guangzhou Institute of Geochemistry, Chinese Academy of Sciences, Guangzhou 510640, P. R. China*

[c]*Graduate University of the Chinese Academy of Sciences, Beijing 100039, P. R. China*

† Electronic supplementary information (ESI) available. See DOI: 10.1039/c7ra09328d

‡ These authors contributed equally to this work.

examined the changes in paddy soil microbial community diversity and abundance during NRCFO at circumneutral pH and found that *Azospira*, *Zoogloea*, and *Dechloromonas* species predominated during NO_3^- reduction in the presence of Fe(II) after addition of lactate.[19] However, neutrophilic NRCFO species from paddy soils have not been reported, and the mechanisms underlying this process have been largely overlooked.

In the present study, we isolated *Rhodocyclaceae* sp. strain Paddy-1 from rice paddy soil. Strain Paddy-1 was capable of NRCFO in the presence of acetate. The kinetics of NO_3^- reduction and Fe(II) oxidation and mineralogy of Fe(III) oxides produced by this microorganism were characterized. We compared the draft genome sequence of Paddy-1 to the genomic information of other NRCFO species. We also predicted the metabolic potential of NRCFO based on annotation of gene function. Our findings provide insight into the mechanisms of NRCFO in microorganisms from soil ecosystems.

2. Experimental section

2.1 Microorganism isolation

Anoxic paddy soil samples were collected at 10 to 20 cm below the soil surface with a wooden spade and preserved in 200 ml sterilized sealed glass bottles (vaccine bottle). The paddy soil fields were located in the South China Botanical Garden of the Chinese Academy of Science in the city of Guangzhou. The geochemical properties of the paddy soil were as follows: pH, 5.96; organic matter content, 41.0 g kg^{-1}; total Fe, 27.9 g kg^{-1}; dithionite/citrate/bicarbonate-extractable Fe concentration, 17.9 g kg^{-1}; amorphous Fe concentration, 4.85 g kg^{-1}; complex Fe concentration (extracted with alkaline sodium pyrophosphate at pH 8.5), 1.13 g kg^{-1}; and other acid extractable elements, Ca^{2+} (0.965 g kg^{-1}), Mg^{2+} (1.08 g kg^{-1}), K^+ (6.66 g kg^{-1}), and Na^+ 0.49 g kg^{-1}. Subsequent procedures were carried out in a DG250 anaerobic workstation (Don Whitley Scientific, West Yorkshire Shipley, UK). 1 g sample of paddy soil core interval was added to 50 ml anoxic (80 : 20 N_2 : CO_2 headspace atmosphere) 10 mM piperazine-*N*,*N*-bis(2-ethanesulfonic acid) (PIPES)-buffered basal medium (pH 7.0) containing 0.2 ml l^{-1} of a micronutrient with the following composition (final concentrations, mg l^{-1}): $FeCl_3 \cdot 4H_2O$ (2), $CoCl_2 \cdot 6H_2O$ (0.01), $MnCl_2 \cdot 4H_2O$ (0.05), $AlCl_3 \cdot 6H_2O$ (2), $CuCl_2 \cdot 2H_2O$ (0.03), $ZnCl_2$ (0.05), H_3BO_3 (0.05), $(NH_4)_6Mo_7O_{24} \cdot 4H_2O$, $Na_2SeO_3 \cdot 5H_2O$ (0.05), $NiCl_2 \cdot 6H_2O$ (0.05), EDTA (1), and resazurin (0.2). The pH of the medium was adjusted to 7.0 using 36% HCl; the medium was prepared without sulfide. A vitamin mixture containing (final concentrations, mg l^{-1}): biotin (2), folic acid (2), pyridoxine hydrochloride (10), riboflavin (5), thiamine (5), nicotinic acid (5), pantothenic acid (5), B-12 (0.1), *p*-aminobenzoic acid (5), and thioctic acid (5) was also added to the culture (5 ml per liter of enrichment medium). This basal medium contained 5 mM $FeCl_2 \cdot 4H_2O$ and 10 mM $NaNO_3$ as the electron donor and acceptor, respectively. Acetate (5 mM) was used as an additional carbon source. After 7 days of incubation in the anaerobic workstation at 30 °C, samples were transferred to fresh liquid medium (1 : 10 dilution) and incubated for 1 week for cell enrichment. The suspension was diluted at ratios of 1 : 10, 1 : 100, and 1 : 1000 in sterile PIPES-buffered basal medium and coated onto solid medium (prepared by mixing 2% agar with the liquid medium). The plates were then incubated in the anaerobic workstation at 30 °C for 7 days to allow formation of heterotrophic colonies. Those showing Fe(II)-oxidizing capacity—as identified by the presence of brownish-red or brownish-green Fe(III) oxide precipitates on or around the colonies—were selected and transferred to fresh anoxic PIPES-buffered liquid medium; one isolated strain (Paddy-1) showing Fe(II)-oxidizing capacity was selected for further characterization.

2.2 DNA extraction and 16S rRNA sequence analysis

Late log-phase cultures of strain Paddy-1 were grown on 5 mM acetate and 10 mM NO_3^-, harvested by centrifugation (6000 ×*g*, 10 min), and washed twice with 20 mM PIPES buffer (pH 7.0). Paddy-1 genomic DNA was extracted using the EZNA Bacterial DNA kit (Omega Bio-Tek, Norcross, GA, USA), and the quality was evaluated by agarose gel electrophoresis. DNA concentration was measured using the Quant-iT dsDNA BR assay kit (Invitrogen, Inchinnan Business Park, UK) according to the manufacturer's instructions, and the sample was used as a template in PCR amplification of the 16S rRNA gene with the 27F and 1492R universal primers and the following cycling program: 95 °C for 5 min; 30 cycles of 94 °C for 30 s, 55 °C for 1 min, and 72 °C for 30 s; and 72 °C for 1.5 min.[20] The PCR product was purified using the DNA Gel Extraction kit (Omega Bio-Tek) and cloned into the pGEM-T vector (Promega, Madison, WI, USA), which was then transformed into *Escherichia coli* JM109 competent cells. Sequencing was performed on a 3730 DNA Analyzer (Applied Biosystems, Foster City, CA, USA). A BLAST search of the sequence assembled using Bioedit software[21] was performed against the National Center for Biotechnology Information (NCBI) database and the Ribosomal Database Project.[22] The purity of the culture was assessed using the 16S rRNA gene clone library; 20 randomly chosen clones showed 100% sequence similarity with one another. Sequence results with a high similarity were edited, and a phylogenetic tree was constructed by the neighbor-joining method using MEGA 4.0 software.[23] Identification of Paddy-1 to the species level was performed using EzBioCloud.[24]

2.3 Analysis of Fe(II) oxidation and NO_3^- reduction by strain Paddy-1

The stoichiometry of Fe(II) oxidation and NO_3^- reduction was determined using three tubes of medium inoculated with strain Paddy-1 at a cell density of approximately 5.5 × 10^6 cells per mm. The cells were harvested by centrifugation at 6000 ×*g* for 10 min, washed twice with anaerobic 20 mM PIPES buffer (pH 7.0), and resuspended for experiments conducted under the following conditions: (1) cells with 10 mM NO_3^- and 5 mM $FeCl_2$ representing biotic NRCFO; (2) 10 mM NO_3^- and 5 mM $FeCl_2$, an abiotic control for NRCFO; (3) cells with 5 mM $FeCl_2$, a negative control for Fe(II) oxidation during cell growth; (4) cells with 10 mM NO_3^-, a biotic NO_3^- reduction reaction; (5) cells

with 1 mM NO_2^- and 5 mM $FeCl_2$, an abiotic reaction of NO_2^- and Fe(II) in the presence of active cells; (6) 5 mM NO_2^- and 5 mM $FeCl_2$, an abiotic reaction between NO_2^- and Fe(II); and (7) cells with 5 mM NO_2^-, a biotic NO_2^- reduction reaction. The culture conditions for evaluation of NO_3^- reduction and Fe(II) oxidation by strain Paddy-1 were similar to those of organism isolation, in which the strain was incubated in anoxic PIPES at 30 °C and simultaneously supplied with micronutrients and vitamins. In each treatment, 5 mM acetate was added as a carbon substrate. After 0, 1, 2, 3, 4, and 6 days, samples were collected to examine changes in the concentrations of nitrogen and iron species during incubation. In addition, 20 mM sodium azide (NaN_3), an inhibitor of bacterial growth, was added at the mid-late log phase of growth (2 days) in the NRCFO experiments as a control to verify that the presence of active cells was necessary for Fe(II) oxidation.

NO_3^- and NO_2^- concentrations were determined at specified time intervals by ion chromatography as previously described.[25] Initial concentrations of $FeCl_2 \cdot 4H_2O$ and $NaNO_3$ were 5 and 10 mM, respectively. N_2O in the culture headspace was quantified by gas chromatography combined with mass spectrometry.[26] Ammonium concentration was determined using a San^{++} continuous flow analyzer (Skalar Analytical B.V., Breda, The Netherlands). For quantification of Fe(II) and Fe(III), samples were immediately transferred to 40 mM sulfamic acid solution to prevent chemical Fe(II) oxidation. After dissolution, the concentration of Fe(II) in ferrozine was measured spectrophotometrically at 562 nm.[3] Total iron content was determined by reducing an aliquot of the sample with hydroxylamine hydrochloride prior to adding ferrozine reagent. Fe(III) concentration was calculated by subtracting the amount of Fe(II) from the total iron amount. All measurements in the ferrozine assay were performed in triplicate. Cell growth was monitored by detecting changes in the protein concentration with the Bradford assay using bovine serum albumin as the standard.[27] Acetate was quantified by ion chromatography with conductivity detection (IonPacAS9-HC analytical column and DX-500 system; Dionex, Sunnyvale, CA, USA). To identify the organic substrates that support growth, we tested the following compounds: fumarate, sucrose, glucose, citrate, lactate, ethanol, and glycerol (5 mM each).

2.4 Analysis of bacterial morphology and mineralogical profile

In an anaerobic workstation, microbially produced Fe(III) precipitate was washed twice with anoxic phosphate-buffered saline (150 mM NaCl aqueous solution containing 0.1 mM EDTA and 20 mM sodium phosphate adjusted to pH 7.0) to remove salts and was then dried in the same workstation. X-ray diffraction (XRD) spectra were obtained on a Scintag Pad V X-ray powder diffractometer (Scintag, Cupertino, CA, USA) using Cu-Kα radiation operating at 35 kV and 30 mA and a θ–2θ goniometer equipped with a germanium solid-state detector. Structures were identified by comparisons to spectra in the PCPDFWIN program, Joint Committee on Powder Diffraction Standards International Centre for Diffraction Data, 1997 (Newton Square, PA, USA) and to the spectra of synthetic lepidocrocite and goethite. Fe(III) precipitate was also characterized by scanning electron microscopy (SEM) coupled with energy dispersive X-ray spectroscopy (EDS) (XFlash 5010; Bruker Daltonik GmbH, Bremen, Germany). Samples were examined with a scanning electron microscope (Super 55VP; Zeiss, Oberkochen, Germany) at accelerating voltages of 15–35 kV. For transmission electron microscopy, 5 ml of culture supernatant was centrifuged, fixed in 2.5–3% (v/v) glutaraldehyde for 12 h at 4 °C and washed three times in water. Half of the samples were stained with 2% osmium tetroxide and 2% uranyl acetate, whereas the other half were left unstained. All of the specimens were dehydrated in ethanol and acetone before embedding in Epon resin. After polymerization for 24 h at 60 °C, sample blocks were sectioned at a thickness of 60 nm on a MT-X ultra microtome using a 55° Diatome diamond knife; ultrathin sections were placed on 200-mesh copper grids. The samples were post-stained with 2% uranyl acetate for 3 min prior to imaging.

2.5 Genome sequencing of strain Paddy-1 and comparison of metabolic pathways with those reported in other NO_3^--reducing Fe(II) oxidizers

The strain Paddy-1 genome was sequenced at Macrogen (Seoul, Korea; http://www.macrogen.com) by conventional whole-genome shotgun sequencing with an Illumina HiSeq system. Two genomic libraries with an insert size of 180 and 800 bp were constructed, resulting in 139 604 478 reads with a read length of 101 bp at approximately 4000× genome coverage. Quality reads were assembled using the Velvet assembler.[28] The drafted genome sequence of strain Paddy-1 had 53 contigs with an N50 size of 200 975 bp (length of longest contig: 506 413 bp; number of contigs >1k: 38; total bases in contigs >1k: 3 549 457). Gene identification was performed using Glimmer3 software,[29] yielding 3273 genes with an average length of 960 bp. The tRNAScan-SE tool[30] was used to identify tRNA genes, whereas ribosomal RNA genes were found by searching against models of ribosomal RNA genes generated with SILVA.[31] The average nucleotide identity (ANI) between the complete and draft genome sequences of all NO_3^--reducing Fe(II) oxidizers was determined using JSpecies software with default parameters.[32] The distance matrix based on obtained ANI values was used to construct a neighbor-joining tree in Splitstree.[33] Protein-coding genes were predicted across genome bins using Glimmer3 (ref. 29) and functional prediction of identified open reading frames was performed by similarity searches against the Evolutionary Genealogy of Genes: Non-supervised Orthologous Groups (eggNOG)[34] and Kyoto Encyclopedia of Genes and Genomes (KEGG)[35] databases using an E value of 10^{-5}. Metabolic pathways that were similar among NO_3^--reducing Fe(II) oxidizers were clustered based on gene abundance in eggNOG and KEGG databases after z-score normalization across all genomes. Proteins were also examined as potential candidates for Fe(II) oxidation by comparison to iron-oxidizing proteins in other bacteria such as *Acidithiobacillus ferrooxidans* ATCC23270, *Leptospirillum ferrooxidans* C2_3, *Sideroxydans lithotrophicus* ES-1, *Rhodopseudomonas palustris* tyrosine kinase with immunoglobulin-like and EGF-like domains (TIE)-1, and *Rhodobacter ferrooxidans* SW2 (Table S1†).

2.6 Nucleotide sequence accession number

The 16S rRNA sequences of strain Paddy-1 were deposited in GenBank under the accession number KT322180. The draft genome sequence of strain Paddy-1 was deposited at NCBI under the BioProject ID PRJNA291117.

3. Results

3.1 Enrichment and isolation of strain Paddy-1, an NO_3^--reducing Fe(II) oxidizer

We successfully isolated a novel, anaerobic, neutrophilic, NO_3^--reducing, Fe(II)-oxidizing bacterium from paddy soil. Enrichment cultures with paddy soil were incubated for 7–10 days. The precipitates were identified as ferric iron hydroxides based on their reddish-brown color. Cells of strain Paddy-1 were Gram-negative, rod-shaped, and approximately 2–3 μm in length (Fig. S1†). Phylogenetic analysis of the 16S rRNA gene sequence placed strain Paddy-1 in the family *Rhodocyclaceae* and revealed that it was most closely related to *Azospira oryzae* 1 (GU123605) with 94% sequence similarity (Fig. S2†), followed by the NDFO *A. suillum* PS (AF170348, formally *D. suillum* PS)[17] and *Pseudogulbenkiania* sp. strain 2002 (AY609199) (92% and 86% sequence similarity, respectively).[18]

3.2 NO_3^--reducing Fe(II) oxidation by strain Paddy-1

NO_3^--reducing anaerobic oxidation of Fe(II) by strain Paddy-1 in the presence of acetate is shown in Fig. 1 and 2. The NO_3^- concentration decreased by 97% over the experimental period of NRCFO from 9.28 mM to approximately 0.28 mM after 6 days of incubation (Fig. 1A). NO_2^- accumulation in the culture was observed on day 1 during NO_3^--reduction coupled with Fe(II) oxidation. The NO_2^- concentration increase after day 6 to approximately 1.57 mM (Fig. 1B). Stoichiometrically, the reduction of 9.28 mM NO_3^- should produce 9.28 mM NO_2^-. However, NO_2^- concentration was only 1.57 mM on day 6, suggesting that NO_2^- is further converted to N_2O, N_2, or NH_4^+ by denitrification or by reaction with Fe(II) in the medium. Ammonia concentration ranged from 0.02–0.07 mM in the solution (Fig. 1D), and only trace quantities of N_2O (0.03–0.2 mM) were detected in the headspace over the course of incubation (Fig. 1C), indicating that most of the NO_3^- was eventually converted to N_2.

Fe(II) was oxidized concomitantly with NO_3^- reduction in the presence of acetate (Fig. 2A). During NRCFO, the Fe(II) concentration decreased by 86% from 5.1 mM to approximately 0.7 mM (approximately 0.73 mM per day). In the absence of NO_3^-, there was no Fe(II) oxidation under the same conditions. In addition, no Fe(II) oxidation or NO_3^- reduction was observed during a 6 day incubation in NO_3^- and Fe(II) cultures without cells (Fig. 1 and 2). NaN_3 (20 mM) was added at the mid-late log phases of growth (2 days) in experiments performed with cultured cells, $FeCl_2$, NO_3^-, and acetate. The rate of Fe(II) oxidation and NO_3^- reduction was inhibited by NaN_3, implying that active cells are necessary for Fe(II) oxidation (Fig. 1 and 2). Between days 1 and 6, 0.30–1.57 mM NO_2^- accumulated following NO_3^- reduction in the NRCFO experiments that accelerated Fe(II) oxidation. Abiotic control experiments also showed rapid reactions between ~5 mM NO_2^- and ~5 mM $FeCl_2$ after 6 days (Fig. 1 and 2), suggesting that the high NO_2^- concentration contributed to Fe(II) oxidation in cultures with strain Paddy-1. N_2O (0.03–0.21 mM) and NH_4^+ (0.02–0.07 mM)

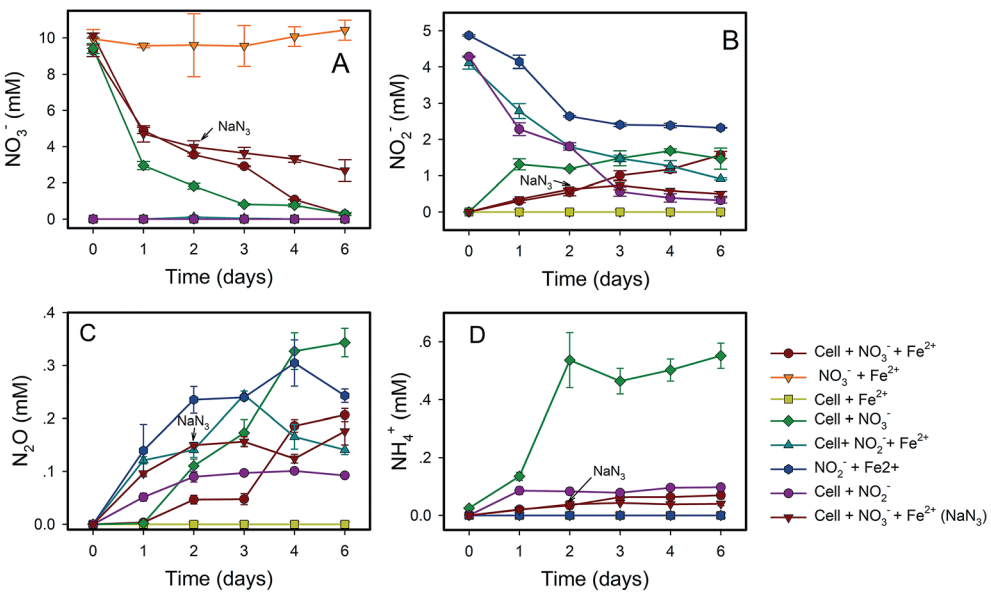

Fig. 1 Transformations of nitrate (A), nitrite (B), nitrous oxide (C) and ammonium (D) by (1) *Rhodocyclaceae* sp. strain Paddy-1 (~10^9 cells per ml) with 10 mM NO_3^- and 5 mM $FeCl_2$; (2) 10 mM NO_3^- and 5 mM $FeCl_2$; (3) cells with 5 mM $FeCl_2$; (4) cells with 10 mM NO_3^-; (5) cells with 1 mM NO_2^- and 5 mM $FeCl_2$; (6) 5 mM NO_2^- and 5 mM $FeCl_2$; (7) cells with 5 mM NO_2^-; (8) 20 mM NaN_3 was added at the mid-late log phase of growth (2 days) during the NRCFO experiments. In each treatment, 5 mM acetate was added as a carbon substrate. Data were all presented as means ± standard deviations (SD) of triplicate. When not shown, error bars are smaller than the symbol size.

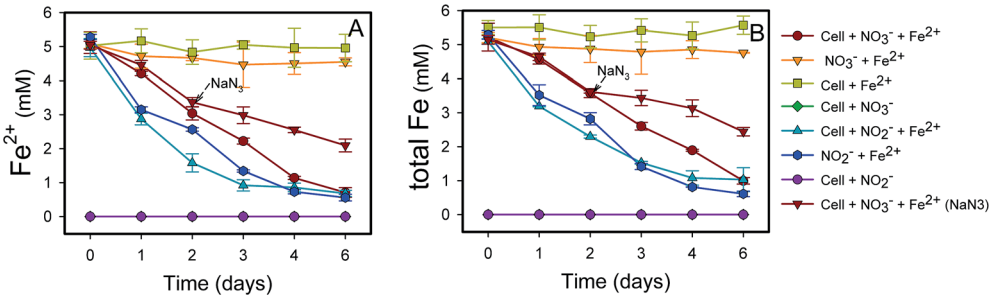

Fig. 2 Transformations of dissolved Fe(II) (A) and total Fe (B) by (1) *Rhodocyclaceae* sp. strain Paddy-1 (~10^9 cells per ml) with 10 mM NO_3^- and 5 mM $FeCl_2$; (2) 10 mM NO_3^- and 5 mM $FeCl_2$; (3) cells with 5 mM $FeCl_2$; (4) cells with 10 mM NO_3^-; (5) cells with 1 mM NO_2^- and 5 mM $FeCl_2$; (6) 5 mM NO_2^- and 5 mM $FeCl_2$; (7) cells with 5 mM NO_2^-; (8) 20 mM NaN_3 was added at the mid-late log phase of growth (2 days) during the NRCFO experiments. In each treatment, 5 mM acetate was added as a carbon substrate. Data were all presented as means ± standard deviations (SD) of triplicate. When not shown, error bars are smaller than the symbol size.

accumulation was clearly lower in the presence of cells along with Fe(II) and NO_3^- than that observed in a control experiment with cells and NO_3^- only (N_2O 0.02–0.34 mM, NH_4^+ 0.03–0.55 mM) (Fig. 1D). In addition, Fe(II) addition appeared to slightly inhibit the reduction of NO_3^-. Acetate (5 mM) was completely oxidized by strain Paddy-1 in the presence of 10 mM NO_3^- and 5 mM Fe(II) after incubation for 4 days (Fig. 3). Adding NaN_3 inhibited acetate oxidation during NRCFO (Fig. 3). Moreover, the consumption of acetate was much lower under NRCFO than under biotic NO_3^--reducing conditions alone, indicating that the contribution of acetate as an electron donor was diminished and that the electron transferred to NO_3^- was partly derived from Fe(II) under NRCFO conditions.

Most NO_3^--reducing Fe(II) oxidizers isolated to date require organic substrates for growth.[15,17,26,36] In addition to acetate, alternative carbon sources such as formate, glucose, sucrose, glycerol, alcohol, and citrate may be utilized by strain Paddy-1 under anoxic conditions (Fig. S3†). However, lactate cannot be used by this strain, suggesting that it is a mixotrophic bacterium that can utilize inorganic Fe(II) or organic acid as an electron donor. The respiratory pathways of various carbon sources (included lactate, formate, glucose, sucrose, glycerol, alcohol and citrate) in strain Paddy-1 may produce different amount of energy and impact the cellular activities, resulting in the rate variation of Fe(II) oxidation.

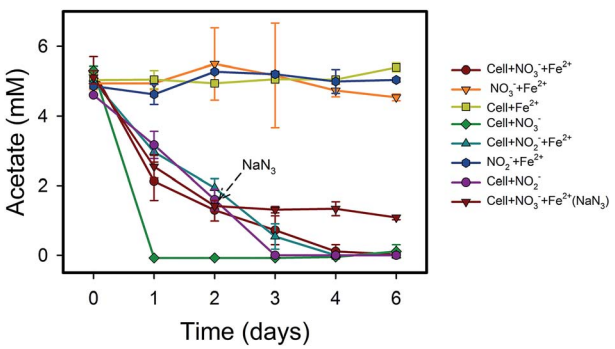

Fig. 3 The oxidation of acetate by (1) *Rhodocyclaceae* sp. strain Paddy-1 (~10^9 cells per ml) with 10 mM NO_3^- and 5 mM $FeCl_2$; (2) 10 mM NO_3^- and 5 mM $FeCl_2$; (3) cells with 5 mM $FeCl_2$; (4) cells with 10 mM NO_3^-; (5) cells with 1 mM NO_2^- and 5 mM $FeCl_2$; (6) 5 mM NO_2^- and 5 mM $FeCl_2$; (7) cells with 5 mM NO_2^-; (8) 20 mM NaN_3 was added at the mid-late log phase of growth (2 days) during the NRCFO experiments. In each treatment, 5 mM acetate was added as a carbon substrate. Data were all presented as means ± standard deviations (SD) of triplicate. When not shown, error bars are smaller than the symbol size.

3.3 Fe(III) oxyhydroxide formation and characterization

The mineralogical characteristics of biogenic iron oxidation products of strain Paddy-1 were examined by XRD and SEM-EDS. The broad background peaks present in the XRD spectrum suggested that poorly crystalline Fe(III) oxides were produced by strain Paddy-1 (Fig. S4†), consistent with the XRD analysis of Fe(III) precipitates generated by other NRCFO species.[16,37] Amorphous iron oxides were observed on the cell surface of strain Paddy-1 and no crystalline iron oxides were detected by SEM (Fig. 4A). SEM analysis also revealed aggregates of cells that were encrusted with oxide precipitates after 20 days of incubation in the presence of Fe(II) plus acetate and NO_3^-. High peaks of iron and oxygen were observed in the SEM-EDS images (Fig. 4A), indicating that ferric iron oxyhydroxides are the main oxidation products.

3.4 Genome properties of strain Paddy-1 and metabolic pathways compared to other NO_3^--reducing Fe(II)-oxidizing species

The draft genome of Paddy-1 was 3 554 565 bp in length, which was similar to those of other anaerobic NRCFO species such as *Acidovorax* sp. BoFeN1 (4.0 Mbp), *A. ebreus* TPSY (3.8 Mbp), *A. delafieldii* 2AN (3.8 Mbp), and *Pseudogulbenkiania* sp. 2002 (4.2 Mbp) (Fig. 5). The genome was found to encode 3153 protein-encoding genes, three ribosomal operons, and 50 tRNA genes.

The average GC content of seven NO_3^--reducing Fe(II) oxidizer genomes ranged from 63.8–64.8%. The evolutionary relatedness of NO_3^--reducing Fe(II) oxidizers was examined by calculating the ANI among genomes. The phylogenetic tree based on pairwise comparison of ANI values confirmed the relatedness of strain Paddy-1 to the other NO_3^--reducing Fe(II) oxidizers (Fig. 5), and is consistent with previously determined phylogenies based on 16S rRNA gene sequences (Fig. S2†). ANI

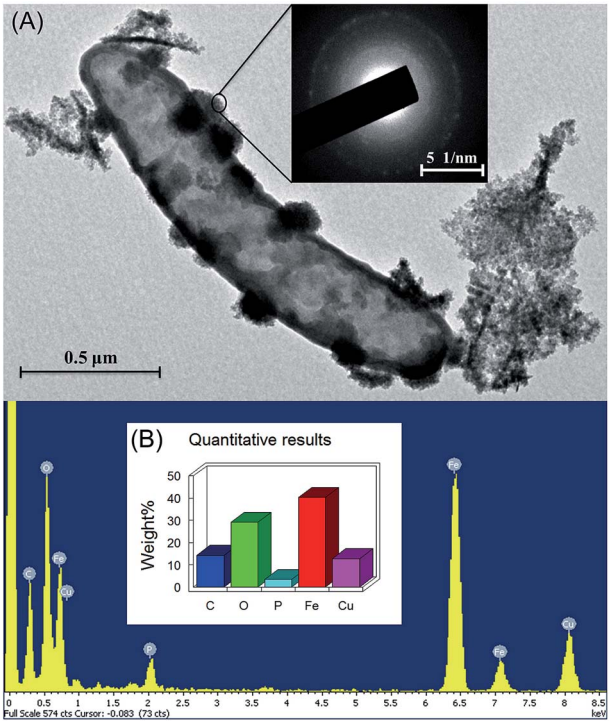

Fig. 4 Scanning electron microscope (SEM) photographs and transmission electron micrographs (TEM) and energy dispersive X-ray spectrometry (EDS) of solids present in the suspension of *Rhodocyclaceae* sp. strain Paddy-1 in the presence of 10 mM nitrate, 5 mM $FeCl_2$ and 5 mM acetate at day 24 of incubation time. (A) Topography of a single cell with uniform Fe(III) oxyhydroxide encrustations after 12 h of incubation; (B) EDS analysis of *Rhodocyclaceae* sp. strain Paddy-1. Vertical line indicates the characteristic peak position of the element. Peak area represents the content of the element.

values among known NO_3^--reducing Fe(II) oxidizers ranged from 67.2–84.1% (Fig. S5†). The genome of strain Paddy-1 was most similar to that of *A. suillum* PS, with an ANI of 76.3, and had ANI values ranging from 78.2% to 84.4% with respect to other NO_3^--reducing Fe(II) oxidizers in the genus *Acidovorax* (*Acidovorax* sp. BeFeN1, *A. delafieldii* 2AN, and *A. ebreus* TPSY) (Fig. 5 and S5†).

To compare the metabolic pathways of NO_3^--reducing Fe(II)-oxidizing species, open reading frames (ORFs) were annotated based on Blastx analyses against the eggNOG and KEGG databases. The number of predicted ORFs in these species ranges from 2770 to 4061 with an average of 3943, corresponding to a coding density in the draft genome of 87.2% ± 4.1% (average ± SD) (Fig. 5). On average, 80.6% (range: 61.3–90.5%) and 47.5% (range: 38.1–9.5%) of ORFs were annotated in the eggNOG and KEGG databases. The results showed that the functional composition of genes was similar across genomes, with function unknown (simplified as [S], average ± SD: 27.2% ± 1.3%), amino acid metabolism and transport ([E], 7.0% ± 1.4%), energy production and conversion ([C], 6.8% ± 0.2%), inorganic ion transport and metabolism ([P], 6.6% ± 0.6%), signal transduction ([T], 6.4% ± 1.7%), and cell wall/membrane/envelop biogenesis ([M], 5.5% ± 0.9%) as the dominant orthologous groups in the eggNOG categories (Fig. S6†). There was greater divergence in the functional composition of KEGG as compared to eggNOG categories among genomes, with functions associated with amino acid metabolism (average ± SD: 12.0% ± 1.1%) being the most abundant, followed by carbohydrate metabolism (10.1% ± 0.4%) and energy metabolism (10.0% ± 0.6%) (Fig. S7†). Most detected functions were common to all genomes, suggesting similarities in the metabolic capabilities of different NO_3^--reducing Fe(II) oxidizers. In particular, eggNOG and KEGG functional clustering showed more similarity between the genomes of strain Paddy-1 and *A. suillum* PS (Fig. S8 and S9†), whereas the other NO_3^--reducing Fe(II)-oxidizing species (*Acidovorax* sp. BeFeN1, *A. delafieldii* 2AN, and *A. ebreus* TPSY) belonging to genus *Acidovorax* were grouped together. These patterns were similar to the results obtained in the phylogenetic

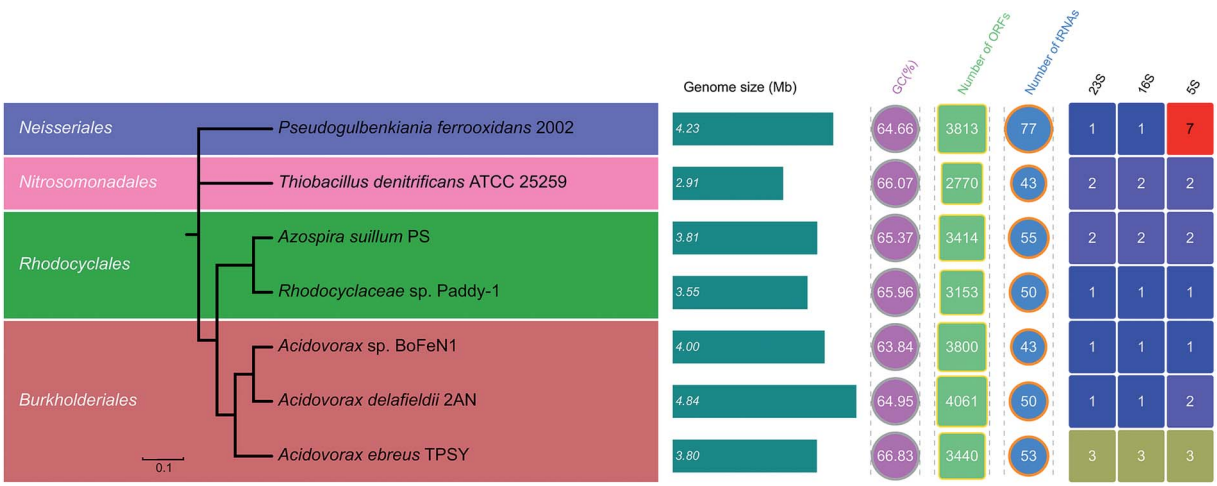

Fig. 5 Average nucleotide identity (ANI)-based neighbor-joining tree and genome features of seven sequenced strains capable of nitrate reduction coupled Fe(II) oxidation. The evolutionary relatedness was examined by calculation of ANI, based on draft or complete genome sequences. Scale indicates the % difference ANI.

analysis based on 16S rRNA genes (Fig. S2†) or ANI values (Fig. 5).

Denitrification-related genes. During incubation of strain Paddy-1, the concentration of generated NO_2^- remained at low levels (1.57 mM, Fig. 1B), suggesting that NO_2^- is further converted to N_2O, N_2, or NH_4^+. Genes encoding all of the components of the denitrification pathway were present in the genome of strain Paddy-1, including NO_3^- reductase (nar*G*), NO_2^- reductase (nir*K*), nitric oxide reductase (nor*B*), nitrous oxide reductases (nos*Z*), and ferredoxin–NO_2^- reductase (nir*A*) (Fig. 6). These results are consistent with the change in nitrogen speciation during the process of NO_3^--reducing anaerobic oxidation of ferrous iron by strain Paddy-1 with acetate as substrate.

Iron homeostasis machinery. Unexpectedly, strain Paddy-1 has a large number of iron homeostasis related components, including 41 putative genes encoding (poly)ferredoxin, flavodoxins, bacterioferritin, (proto)heme, and siderophore (Table S3†). These components could ensure iron acquisition and consumption by cells *in vivo*. In addition, iron storage proteins such as ferritin were also present, and could provide intracellular iron reserves when the external supply is restricted. Strain Paddy-1 had nine ORF-encoding Feo*B* transporters that facilitate Fe(II) import into the periplasm; extracellular ferric chelators such as siderophores were also detected. The strain Paddy-1 genome also harbored membrane-integral Fe(II) permease (COG0672, ORF_0429) and ferric reductase (COG4097, ORF_2503, and ORF_1211), which participate in Fe(II) transmembrane transport and Fe(III) reduction, respectively (Table S3†).

Putative genes encoding cytochrome c, iron oxidase, and electron transport chain components for Fe(II) oxidation. Automated annotation of the genome of strain Paddy-1 predicted 31 genes encoding c-type cytochromes or related proteins, two of which were highly homologous to di-heme c-type cytochromes (Table S2†). In addition to these genes, we identified 29 genes encoding or related to *cytochrome c* (including cytochrome *c1*, *c2*, *c5*, *c553*, and *c556*), which plays an important role in electron transfer and exhibits high iron ion-binding capacity. Bioinformatics analyses have enabled the identification of putative electron transport chain components involved in Fe(II) oxidation.[38,39] Manual curation of the Paddy-1 genome revealed a number of high-similarity homologs of iron oxidase or electron transfer proteins in the acidophilic, Fe(II) oxidizer *A. ferrooxidans* 23270 and the dissimilatory Fe(III) reducer *S. oneidensis* MR-1 (Table S4†). A cyc*2* homolog (*E* value $= 3 \times 10^{-33}$) was found in the strain Paddy-1 genome. *Cyc2* gene encodes a cytochrome located in the outer membrane of the cell that catalyzes the oxidation of Fe(II) to Fe(III). Furthermore, homologs of electron transfer complex proteins including cyc*1* (*E* value $= 9.00 \times 10^{-32}$), cyc*A-2* (*E* value $= 2.00 \times 10^{-11}$), and cyc*A-1* (*E* value $= 1.00 \times 10^{-28}$) were also predicted based on the genomic information. In addition, the homologs of Feo*B* (a ferrous iron transport protein) and cym*A* (a hydroquinone dehydrogenase) in *S. oneidensis* MR-1 had *E* values of 8.00×10^{-8} and 1.00×10^{-31}, respectively.[40,41] In *S. oneidensis*, cym*A* is a tetraheme c-type cytochrome that is presumed to localize to the cytoplasmic membrane where it mediates electron transfer from the quinone/quinol pool.[41] We propose that the proteins encoded by these genes are key components of the Fe-oxidizing pathway in strain Paddy-1 (Table S3†).

4. Discussion

4.1 Beneficial effects of poorly crystalline Fe(III) minerals produced by NRCFO species

The microbial Fe(II)–Fe(III) cycle promotes various environmental processes at the water–soil interface, including nutrient cycling and contaminant transformation.[42,43] Fe(II) produced by dissimilatory Fe(III)-reducing bacteria can be re-oxidized to Fe(III) *via* a chemical or biological process to complete the iron cycle. Crystalline Fe(III) minerals produced at lower levels by NRCFO species were shown to act as excellent electron acceptors for dissimilatory Fe(III)-reducing bacteria.[44,45] Fe(III) mineral phases of NRCFO products are often poorly crystalline and their mineralogy is determined by factors such as medium composition, pH, co-substrate concentrations, incubation conditions, Fe(II) oxidation rates, and presence of humic compounds or other ligands.[16,46] In this study, strain Paddy-1 oxidized Fe(II) mixotrophically in the presence of acetate and NO_3^-, forming

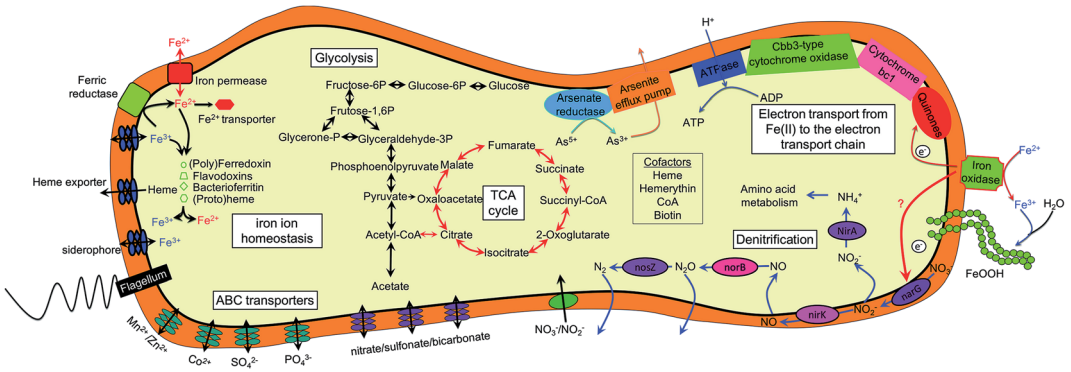

Fig. 6 Cell metabolic cartoon based on the annotation of *Rhodocyclaceae* sp. strain Paddy-1 genome. Possible mechanisms for energetic benefit from nitrate reduction coupled to Fe(II) oxidation in the cell of *Rhodocyclaceae* sp. strain Paddy-1 was shown. narG, nitrate reductase; nirK, nitrite reductase; norB, nitric oxide reductase; nosZ, nitrous oxide reductase; nirA, ferredoxin–nitrite reductase.

Fe(III) mineral crusts around the cell (Fig. 4). The production of poorly crystalline Fe(III) oxides by Paddy-1 was confirmed by XRD (Fig. S4†) and is consistent with observations in other NRCFO species.[37,47–49] These poorly soluble Fe(III) oxides prevent encrustation of metabolizing cells, which can impair substrate uptake and metabolite release and may lead to cell death.[50] Furthermore, the low levels of crystalline Fe(III) produced by NRCFO bacteria may act as nucleation sites to promote the growth of iron oxides with a higher-order crystalline structure,[16,51] and may be transformed into hematite (Fe_2O_3)[52] or decomposed to lower-order species that are transformed into highly crystalline forms such as goethite.[53] In addition to releasing dissolved Fe(II), Fe(III)-reducing bacteria could also catalyze the transformation of poorly ordered Fe(III) hydroxides into higher crystalline Fe(III) minerals *via* a dissolution/re-precipitation mechanism[39] that yields secondary iron minerals such as ferrihydrite, goethite, magnetite, or even carbonated green rust.[54,55] In addition to enhancing iron cycling, poorly crystalline Fe(III) minerals produced by NRCFO species can potentially attenuate environmental contaminants present in rice paddy soils. Less crystalline Fe(III) minerals are more readily utilized by dissimilatory Fe(III)-reducing microorganisms, which can use organic pollutants such as aromatic hydrocarbons as electron donors.[56] They also have a larger surface area that increases their capacity for binding toxic metals such as arsenic and cadmium.[57]

4.2 Abiotic reactions in microbe-mediated NRCFO

Discerning whether biotic or abiotic processes control Fe(II) oxidation remains a major challenge.[1] Fe(II) can be abiotically oxidized by Mn(III)/Mn(IV) oxide, copper, and green rust.[26,54,55,58,59] The indirect abiotic process of Fe(II) oxidation may be driven by heterotrophic NO_3^--reducing bacteria *via* reactive nitrogen (N) species (NO_2^-, NO) generated by denitrification.[54] Analysis of nitrogen species in strain Paddy-1 cultures with $FeCl_2$ and NO_3^- showed that the NO_2^- concentration was <1 mM after 3 days when Fe(II) was rapidly oxidized (Fig. 1 and 2). NO_2^- accumulation (~0.5–1.5 mM) in cultures has been reported in other NRCFO studies.[14,16,60] The kinetics of Fe(II) oxidation by NO_2^- are generally more rapid under anoxic conditions,[61,62] with the slowest reaction rate observed at neutral pH. In this study, 20 mM NaN_3 was added at the mid-late log growth phase in the NRCFO experiments as a control to confirm that active cells must be present for Fe(II) oxidation. NaN_3 can inhibit cell growth and metabolic activity.[63] Fe(II) oxidation and NO_3^- reduction rates were reduced by NaN_3 relative to their no-NaN_3 NRCFO counterparts, implying that NRCFO is mediated by active cells (Fig. 1 and 2). The slower consumption of acetate under NRCFO as compared to biotic NO_3^--reducing conditions (Fig. 3) indicated that the contribution of acetate as an electron donor was reduced and that the electron transferred to NO_3^- was partly derived from Fe(II) through NRCFO.

The kinetics and reaction pathways of Fe(II) oxidation by NO_2^- are strongly affected by medium composition, pH, reactant concentration, and the presence of Fe(II)-sorptive (*e.g.*, Fe(III) oxyhydroxides) and cell surfaces.[64] Fe^{2+} adsorbed on crystalline Fe(III) oxyhydroxides is a stronger reactant for NO_2^- than dissolved Fe^{2+}.[65] It is possible that the abiotic reaction between NO_2^- and Fe^{2+} absorbed on crystalline Fe(III) oxyhydroxides increase the risk of overestimating the microbial contribution to NRCFO. However, Fe(III) oxyhydroxides produced by strain Paddy-1 were poorly crystalline in form, which reduced the possibility that adsorbed Fe(II) would react with generated NO_2^-. Because adsorbed Fe(II) is difficult to distinguish on the surface of cells or Fe(III) oxyhydroxides, it is not possible to evaluated its effect on NO_2^- reduction in a biotic system. Continuous flow systems can limit the absorption of Fe(II) absorbed to the cell or Fe(III) oxyhydroxide surface, thereby minimizing the abiotic reaction between Fe(II) and NO_2^-.[14] Additionally, factors such as substrate concentration and buffer type should be carefully considered in NRCFO studies. Until recently, Fe(II) and NO_3^- concentrations used in these studies were in the mM range, which is much higher than those found in the natural environment. A culture system with low concentrations of substrate (Fe(II), NO_3^-, and acetate) could prevent encrustation by generated Fe(III) oxides and reduce their effects on cellular activity.[14] Iron isotopes have been successfully applied in the study of NO_3^--reducing and photoautotrophic Fe(II)-oxidizing bacteria.[66,67] The distinct iron isotope fractions generated by chemical and biological Fe(II) oxidation could serve as indicators of chemical and biological Fe(II) oxidation in the NRCFO process. Therefore, additional studies are warranted using continuous flow systems combined with iron isotope fractionation under much lower Fe(II) and NO_3^- concentrations to characterize NRCFO by strain Paddy-1.

4.3 Fe(II)-oxidizing pathway predicted from the genomic analysis

Although NRCFO has been reported in many species under various conditions, our understanding of the Fe(II) oxidation pathway in this process remains limited. For instance, the location of Fe(II) oxidase in these cells has not been determined.[3] This raises the question of whether Fe(II) is taken up by cells and oxidized in the periplasm or cytoplasm, or whether electrons are transferred from Fe(II) to the outer cell membrane. The cellular and biochemical evidence for the existence of enzymatic NO_3^--reducing Fe(II) oxidation is inconclusive due to the lack of an efficient gene knockout system in these microorganisms. Genome sequencing of several NRCFO species such as *A. ebreus* TPSY,[15] *T. denitrificans* ATCC 25259,[38] and *Pseudogulbenkiania* sp. 2002 (ref. 68) has provided insight into the potential biochemical and genetic mechanisms of NDFO. Initial oxidation of Fe(II) to Fe(III) is performed by Fe(II) oxidase present on the cell surface or in the outer membrane in acidophilic and photosynthetic Fe(II) oxidizers,[69,70] which can prevent Fe(III) mineral precipitation within the cell. Comparative genomics have revealed Fe(II) oxidation factors in microaerophilic species[39,71] including Cyc2 in acidophilic *A. ferrooxidans*,[72] Pio*A*/*B* in photoferrotrophic *R. palustris* TIE-1,[70] Fox*E* in *Rhodobacter* sp. SW2,[73] and Mto*A* in microaerobic *S. lithotrophicus* ES-1.[39] However, iron oxidases in NRCFO species remain poorly

understood.[12] In this study, we found that the genome of strain Paddy-1 encodes a homolog of *A. ferrooxidans* Cyc2—which is located on the outer cell membrane and directly catalyzes Fe(II) oxidation[72]—along with homologs of component of the electron-conducting super-complex spanning the outer and inner membranes of the cytoplasm (cyc*1*, cyc*A1* and cyc*A2* in *A. ferrooxidans*) (Table S4†). Enzymatic assays to determine the localization of the Fe(II) oxidase activity of NRCFO species is necessary in order to elucidate the molecular mechanism of NRCFO in microorganisms. In addition, newly developed proteomics tools such as isobaric tags for relative and absolute quantitation-labeling protein quantification[74] and sequential windowed acquisition of all theoretical fragment ion mass spectra[75] are useful for identifying proteins that participate in electron transfer in the NRCFO process and clarifying the role of c-type cytochromes in Fe(II) oxidation.

5. Conclusions

Anaerobic NRCFO has been observed in anoxic freshwater and sediment environments. However, *in situ* NRCFO in paddy soil—the most widely distributed and constructed wetland system worldwide—has not been previously reported. In this study, we isolated the NRCFO strain Paddy-1 from paddy soil located in iron-rich Southern China and performed whole-genome sequencing to identify some of its critical metabolic components. Additional studies are necessary to determine whether abiotic or biotic reactions are more abundant in the microbe-mediated NRCFO process; moreover, proteins that directly catalyze Fe(II) oxidation in NRCFO species warrant more detailed investigation by proteomics and high-throughput genetic analyses using a systems biology approach.

Conflicts of interest

There are no conflicts to declare.

Acknowledgements

This work was supported by the NSFC-Guangdong Joint Fund (U1401234), National Science Foundation of China (No. 41330857, 41201253), the National Key Technology R&G Program of China (2015BAD05B05), Guangdong Key Technologies R&D Program (2015B020207001) and Natural Science Foundation of Guangdong Province (2017A030313218). We thank Tiffany Louie for thoughtful reviews of the manuscript and discussion of the topics therein.

References

1 E. D. Melton, E. D. Swanner, S. Behrens, C. Schmidt and A. Kappler, *Nat. Rev. Microbiol.*, 2014, **12**, 797–808.
2 L. J. Ding, X. L. An, S. Li, G. L. Zhang and Y. G. Zhu, *Environ. Sci. Technol.*, 2014, **48**, 10641–10647.
3 N. Klueglein and A. Kappler, *Geobiology*, 2013, **11**, 180–190.
4 K. J. Edwards, D. R. Rogers, C. O. Wirsen and T. M. McCollom, *Appl. Environ. Microbiol.*, 2003, **69**, 2906–2913.
5 D. Emerson and C. L. Moyer, *Appl. Environ. Microbiol.*, 2002, **68**, 3085–3093.
6 R. E. James and F. G. Ferris, *Chem. Geol.*, 2004, **212**, 301–311.
7 D. Kanaparthi, B. Pommerenke, P. Casper and M. G. Dumont, *ISME J.*, 2013, **7**, 1582–1594.
8 D. Sobolev and E. E. Roden, *Geomicrobiol. J.*, 2004, **21**, 1–10.
9 K. Laufer, H. Røy, B. B. Jørgensen and A. Kappler, *Appl. Environ. Microbiol.*, 2016, **82**, 6120–6131.
10 S. Ratering and S. Schnell, *Environ. Microbiol.*, 2001, **3**, 100–109.
11 K. R. Reddy, W. H. Patrick and F. E. Broadbent, *Crit. Rev. Environ. Sci. Technol.*, 1984, **13**, 273–309.
12 M. Ilbert and V. Bonnefoy, *Biochim. Biophys. Acta, Bioenerg.*, 2013, **1827**, 161–175.
13 C. Achtnich, F. Bak and R. Conrad, *Biol. Fertil. Soils*, 1995, **19**, 65–72.
14 A. Chakraborty, E. E. Roden, J. Schieber and F. Picardal, *Appl. Environ. Microbiol.*, 2011, **77**, 8548–8556.
15 K. G. Byrne-Bailey, K. A. Weber, A. H. Chair, S. Bose, T. Knox, T. L. Spanbauer, O. Chertkov and J. D. Coates, *J. Bacteriol.*, 2010, **192**, 1475–1476.
16 A. Kappler, B. Schink and D. K. Newman, *Geobiology*, 2005, **3**, 235–245.
17 J. G. Lack, S. K. Chaudhuri, R. Chakraborty, L. A. Achenbach and J. D. Coates, *Microb. Ecol.*, 2002, **43**, 424–431.
18 K. A. Weber, J. Pollock, K. A. Cole, S. M. O'Connor, L. A. Achenbach and J. D. Coates, *Appl. Environ. Microbiol.*, 2006, **72**, 686–694.
19 X. M. Li, W. Zhang, T. X. Liu, L. X. Chen, P. C. Chen and F. B. Li, *Soil Biol. Biochem.*, 2016, **94**, 70–79.
20 M. F. Polz and C. M. Cavanaugh, *Appl. Environ. Microbiol.*, 1998, **64**, 3724–3730.
21 T. A. Hall, *Nucleic Acids Symp. Ser.*, 1999, **41**, 95–98.
22 J. R. Cole, B. Chai, T. L. Marsh, R. J. Farris, Q. Wang, S. A. Kulam, S. Chandra, D. M. McGarrell, T. M. Schmidt, G. M. Garrity and J. M. Tiedje, *Nucleic Acids Res.*, 2003, **31**, 442–443.
23 K. Tamura, J. Dudley, M. Nei and S. Kumar, *Mol. Biol. Evol.*, 2007, **24**, 1596–1599.
24 O. S. Kim, Y. J. Cho, K. Lee, S. H. Yoon, M. Kim, H. Na, S. C. Park, Y. S. Jeon, J. H. Lee, H. Yi, S. Won and J. Chun, *Int. J. Syst. Evol. Microbiol.*, 2012, **62**, 716–721.
25 D. Connolly and B. Paull, *Anal. Chim. Acta*, 2001, **441**, 53–62.
26 K. L. Straub, M. Benz, B. Schink and F. Widdel, *Appl. Environ. Microbiol.*, 1996, **62**, 1458–1460.
27 N. Kruger, in *The Protein Protocols Handbook*, ed. J. Walker, Humana Press, 2009, ch. 4, pp. 17–24, DOI: 10.1007/978-1-59745-198-7_4.
28 D. R. Zerbino and E. Birney, *Genome Res.*, 2008, **18**, 821–829.
29 A. L. Delcher, K. A. Bratke, E. C. Powers and S. L. Salzberg, *Bioinformatics*, 2007, **23**, 673–679.
30 T. M. Lowe and S. R. Eddy, *Nucleic Acids Res.*, 1997, **25**, 0955–0964.

31 E. Pruesse, C. Quast, K. Knittel, B. M. Fuchs, W. Ludwig, J. Peplies and F. O. Glöckner, *Nucleic Acids Res.*, 2007, **35**, 7188–7196.
32 M. Richter and R. Rosselló-Móra, *Proc. Natl. Acad. Sci. U. S. A.*, 2009, **106**, 19126–19131.
33 D. H. Huson, *Bioinformatics*, 1998, **14**, 68–73.
34 J. Huerta-Cepas, D. Szklarczyk, K. Forslund, H. Cook, D. Heller, M. C. Walter, T. Rattei, D. R. Mende, S. Sunagawa, M. Kuhn, L. J. Jensen, C. von Mering and P. Bork, *Nucleic Acids Res.*, 2016, **44**, D286–D293.
35 M. Kanehisa and S. Goto, *Nucleic Acids Res.*, 2000, **28**, 27–30.
36 M. Benz, A. Brune and B. Schink, *Arch. Microbiol.*, 1998, **169**, 159–165.
37 B. H. Li, C. Y. Tian, D. Y. Zhang and X. L. Pan, *Geomicrobiol. J.*, 2013, **31**, 138–144.
38 H. R. Beller, P. Zhou, T. C. Legler, A. Chakicherla, S. Kane, T. E. Letain and P. A. O'Day, *Front. Microbiol.*, 2013, **4**, 249.
39 J. Liu, Z. Wang, S. M. Belchik, M. J. Edwards, C. Liu, D. W. Kennedy, E. D. Merkley, M. S. Lipton, J. N. Butt, D. J. Richardson, J. M. Zachara, J. K. Fredrickson, K. M. Rosso and L. Shi, *Front. Microbiol.*, 2012, **3**, 37.
40 C. D. Cordova, M. F. Schicklberger, Y. Yu and A. M. Spormann, *J. Bacteriol.*, 2011, **193**, 2312–2321.
41 C. R. Myers and J. M. Myers, *J. Bacteriol.*, 1997, **179**, 1143–1152.
42 T. Borch, R. Kretzschmar, A. Kappler, P. V. Cappellen, M. Ginder-Vogel, A. Voegelin and K. Campbell, *Environ. Sci. Technol.*, 2010, **44**, 15–23.
43 P. W. Boyd and M. J. Ellwood, *Nat. Geosci.*, 2010, **3**, 675–682.
44 A. Kappler and K. L. Straub, *Rev. Mineral. Geochem.*, 2005, **59**, 85–108.
45 K. L. Straub and B. E. E. Buchholz-Cleven, *Appl. Environ. Microbiol.*, 1998, **64**, 4846–4856.
46 M. Nordhoff, C. Tominski, M. Halama, J. M. Byrne, M. Obst, S. Kleindienst, S. Behrens and A. Kappler, *Appl. Environ. Microbiol.*, 2017, **83**, e00752-17.
47 S. Park, D. H. Kim, J. H. Lee and H. G. Hur, *FEMS Microbiol. Ecol.*, 2014, **90**, 68–77.
48 K. L. Straub, W. A. Schönhuber, B. E. E. Buchholz-Cleven and B. Schink, *Geomicrobiol. J.*, 2004, **21**, 371–378.
49 L. D. Zhao, H. L. Dong, R. Kukkadapu, A. Agrawal, D. Liu, J. Zhang and R. E. Edelmann, *Geochim. Cosmochim. Acta*, 2013, **119**, 231–247.
50 R. Hallberg and F. G. Ferris, *Geomicrobiol. J.*, 2004, **21**, 325–330.
51 S. Glasauer, P. G. Weidler, S. Langley and T. J. Beveridge, *Geochim. Cosmochim. Acta*, 2003, **67**, 1277–1288.
52 E. Mendelovici, R. Villalba and A. Sagarzazu, *Mater. Res. Bull.*, 1982, **17**, 241–249.
53 N. Yee, S. Shaw, L. G. Benning and T. H. Nguyen, *Am. Mineral.*, 2006, **91**, 92–96.
54 M. Etique, F. P. A. Jorand, A. Zegeye, B. Grégoire, C. Despas and C. Ruby, *Environ. Sci. Technol.*, 2014, **48**, 3742–3751.
55 C. Pantke, M. Obst, K. Benzerara, G. Morin, G. Ona-Nguema, U. Dippon and A. Kappler, *Environ. Sci. Technol.*, 2012, **46**, 1439–1446.
56 J. M. Zachara, R. K. Kukkadapu, J. K. Fredrickson, Y. A. Gorby and S. C. Smith, *Geomicrobiol. J.*, 2002, **19**, 179–207.
57 E. M. Muehe, L. Scheer, B. Daus and A. Kappler, *Environ. Sci. Technol.*, 2013, **47**, 8297–8307.
58 H. C. B. Hansen, C. B. Koch, H. Nancke-Krogh, O. K. Borggaard and J. Sørensen, *Environ. Sci. Technol.*, 1996, **30**, 2053–2056.
59 C. J. Ottley, W. Davison and W. M. Edmunds, *Geochim. Cosmochim. Acta*, 1997, **61**, 1819–1828.
60 P. Larese-Casanova, S. B. Haderlein and A. Kappler, *Geochim. Cosmochim. Acta*, 2010, **74**, 3721–3734.
61 D. W. Nelson and J. M. Bremner, *Soil Biol. Biochem.*, 1970, **2**, 1–8.
62 J. T. Moraghan and R. J. Buresh, *Soil Sci. Soc. Am. J.*, 1977, **41**, 47–50.
63 H. C. Lichstein and M. H. Soule, *J. Bacteriol.*, 1944, **47**, 221–230.
64 F. Picardal, *Front. Microbiol.*, 2012, **3**, 112.
65 Y.-L. Tai and B. A. Dempsey, *Water Res.*, 2009, **43**, 546–552.
66 L. R. Croal, C. M. Johnson, B. L. Beard and D. K. Newman, *Geochim. Cosmochim. Acta*, 2004, **68**, 1227–1242.
67 A. Kappler, C. M. Johnson, H. A. Crosby, B. L. Beard and D. K. Newman, *Geochim. Cosmochim. Acta*, 2010, **74**, 2826–2842.
68 K. G. Byrne-Bailey, K. A. Weber and J. D. Coates, *J. Bacteriol.*, 2012, **194**, 2400–2401.
69 V. Bonnefoy and D. S. Holmes, *Environ. Microbiol.*, 2012, **14**, 1597–1611.
70 Y. Q. Jiao and D. K. Newman, *J. Bacteriol.*, 2007, **189**, 1765–1773.
71 S. Kato, M. Ohkuma, D. H. Powell, S. T. Krepski, K. Oshima, M. Hattori, N. Shapiro, T. Woyke and C. S. Chan, *Front. Microbiol.*, 2015, **6**, 1265.
72 A. Yarzábal, G. Brasseur, J. Ratouchniak, K. Lund, D. Lemesle-Meunier, J. A. DeMoss and V. Bonnefoy, *J. Bacteriol.*, 2002, **184**, 313–317.
73 L. R. Croal, Y. Q. Jiao and D. K. Newman, *J. Bacteriol.*, 2007, **189**, 1774–1782.
74 K. Aggarwal, L. H. Choe and K. H. Lee, *Briefings Funct. Genomics*, 2006, **5**, 112–120.
75 X. Zhu, Y. Chen and R. Subramanian, *Anal. Chem.*, 2014, **86**, 1202–1209.

